Physica Medica 57 (2019) 160–168

Contents lists available at ScienceDirect

Physica Medica

journal homepage: www.elsevier.com/locate/ejmp

Original paper

Evaluation of patient positional reproducibility on the treatment couch and its impact on dose distribution using rotating gantry system in scanned carbon-ion beam therapy

Takayuki Kanai[a,b], Wataru Furuichi[c], Shinichiro Mori[a,*]

[a] Research Center for Charged Particle Therapy, National Institute of Radiological Sciences, Chiba, Japan
[b] Department of Radiation Oncology, Yamagata University, Faculty of Medicine, Yamagata, Japan
[c] Accelerator Engineering Corporation, Chiba, Japan

ARTICLE INFO

Keywords:
Carbon-ion beam
Patient setup
Range uncertainty
Rotating gantry system

ABSTRACT

Purpose: The daily variations in patient setup may cause beam range uncertainties. We evaluated the reproducibility of relative position between the patient and the treatment couch throughout the treatment course and assessed its effects on dose distributions when a beam passes through treatment couch using rotating gantry system.

Methods: We enrolled 1023 patients (=13072 fractions) treated by carbon-ion pencil beam scanning therapy. Seven treatment sites including prostate, head and neck, bone and soft tissue, rectum, liver, lung, and pancreas were investigated. Inter-fractional changes in couch position relative to the patient were defined as translational errors. Changes in couch rotation were defined as rotational errors. Treatment planning was performed for 4 patients in each of the treatment sites. Dose distributions were then re-calculated after the couch was shifted according to average, 95th percentile, and maximum values of translational error.

Results: Large positional errors (> 1.5 cm) were observed in 5% of treatment fractions. Positional errors were largest in prostate and pancreas patients, while smallest in head and neck and lung patients. There were no or only small changes in PTV-D95 and CTV-D95 values for almost all treatment sites. Clinically significant changes were observed in the duodenum (difference in D2cc values ranged from −55% to 28% with maximum couch shift) in pancreas treatment.

Conclusions: Although underdosage to the PTV or CTV was limited, significant overdoses to organs at risk were found. The improvement of immobilization technique and appropriate selection of gantry angles could reduce the uncertainties due to changes in patient position.

1. Introduction

In recent years, the number of particle therapy facilities has rapidly increased worldwide [1]. Particle beams have been widely used for cancer treatment since they have physical and biological advantages over photon beams [2,3]. Most carbon-ion beam facilities use a fixed beam port system, excepting two facilities having installed commercially available rotating gantry systems [4–6]. In the future, the use of rotating gantry systems will likely increase [7,8]. The advantage of the rotating gantry is its adjustable beam angle setting, which can improve dose distribution and allow higher treatment throughput. The rotating gantry system also enables us to set beams passing through treatment couch. In order to account for the range variations due to treatment couch, a virtual treatment couch can be used in treatment planning [9]. The position of the virtual couch is usually determined by the position of the actual treatment couch in planning CT acquisition.

However, the relative positions of the treatment couch and the patient vary in each patient setup procedure because patients are manually positioned on the couch. Patient's bodies are registered to the isocenter in every treatment fraction. As a result, variations in the relative position may cause interfractional variations in the treatment couch position and differences between the actual couch position in each treatment fraction and the virtual couch position in the planning CT, possibly causing inaccuracies in the simulated range variation. As far as we know, there are few studies about the setup variations of patients positioned on a treatment couch and its effect on dose

* Corresponding author at: Research Center for Charged Particle Therapy, National Institute of Radiological Sciences, 4-9-1, Anagawa, Inage-ku, Chiba 263-8555, Japan.
E-mail address: mori.shinichiro@qst.go.jp (S. Mori).

https://doi.org/10.1016/j.ejmp.2018.12.013
Received 9 July 2018; Received in revised form 30 November 2018; Accepted 17 December 2018
Available online 09 January 2019

Table 1
Number of patients and treatment fractions.

Treatment site	Number of cases	Number of fractions
Prostate	733	12
B&S	71	16
H&N	130	16
Rectum	28	16
Liver	8	4
Lung	7	4
Lung	10	12
Pancreas	36	12

Abbreviations = B&S: bone and soft tissue sarcoma, H&N: head and neck.

distribution [10].

Here, we evaluated the positional reproducibility between patient and treatment couch throughout the treatment course, and we estimated the dosimetric impact from the uncertainty of the positional reproducibility.

2. Methods and materials

2.1. Patients and treatment workflow

We randomly selected 1023 patient cases treated by carbon-ion pencil beam scanning therapy between January 2014 and May 2017 in our hospital. Since we used a fixed horizontal and vertical beam irradiation system, the treatment couch was rotated to extend the beam angle selection. The rotation angle and the patient positioning were decided by considering both target and organ at risk (OAR) positions. Treatments for prostate, bone and soft tissue sarcoma, head and neck, rectum, liver, lung and pancreas were included (Table 1). For lung treatment, fractionation schemes of 4 fractions and 12 fractions were selected. A total of 13,072 treatment fractions were analyzed.

Therapists made immobilization devices for each patient to improve the positional reproducibility. The patient was positioned in a molded urethane resin cushion (Moldcare®, Alcare, Tokyo, Japan). Low-temperature thermoplastic shells (Shell Fitter®, Kuraray Co., Ltd., Osaka, Japan) were then used to cover the patient and affixed with tape to the bottom of the table. These immobilization devices were used for all patients except for prostate treatment, where only thermoplastic shells were used. Other supplemental immobilization devices were used in some patients, such as vacuum cushions (BlueBAG®; Elekta AB, Stockholm, Sweden and Instapak® quick RT, Sealed Air Co., Charlotte, NC USA). After positioning in the immobilization devices, the patients underwent CT scans for treatment planning.

In daily treatment, the patient entered the treatment room and was positioned on the treatment couch and the immobilization devices were applied. Then the patient was transferred to the isocenter automatically by a selective compliance assembly robot arm (SCARA) [11]. Patient position was adjusted with an automatic patient positioning algorithm [12] and two oblique x-ray images acquired by flat-panel detector systems. After patient alignment was completed, every treatment couch position was recorded in 6 degrees of freedom (3 translations and 3 rotation) in logfiles using a table top coordinate system of the International Electrotechnical Commission (IEC) [13] (Fig. 1). Carbon-ion irradiation was then performed.

2.2. Evaluation of the patient positional reproducibility

We evaluated patient positional reproducibility by translational error and angular error. We first calculated the relative position between the patient and the treatment couch. The isocenter and the origin of the table top coordinate system were considered as representative points of patient and treatment couch, respectively. Treatment couch position relative to patient was calculated as a three-dimensional vector from the isocenter to the origin (Fig. 1). The vector was described in the table top coordinate system. The table top coordinate system was rotated in each fraction because the treatment couch was rotated for accurate patient alignment. Therefore, we had to consider the rotation of the couch for calculating relative couch position. Relative couch position in the ith fraction (v_x^i, v_y^i, v_z^i) was calculated by

$$\begin{pmatrix} v_x^i \\ v_y^i \\ v_z^i \\ 1 \end{pmatrix} = -(A_\varphi^i A_\psi^i A_T^i A_\theta^i) \begin{pmatrix} 0 \\ 0 \\ 0 \\ 1 \end{pmatrix}, \quad (1)$$

where A_φ, A_ϕ, and A_θ represent 4×4 linear transformation matrices that rotate in the ψ_t, ϕ_t, and θ_t directions, respectively, and A_T represents a linear transformation matrix that translates along the x_t, y_t, and z_t axis, respectively (Fig. 1). A detailed derivation of the equation is described in the appendix section. The angular difference (v_ψ^i, v_φ^i, v_θ^i) was calculated by the difference between planned and actual angles.

For evaluating interfractional variation of couch translation and rotation, we calculated translational error and angular error from relative couch position and angular difference, respectively. Translational error (δ_x^i, δ_y^i, δ_z^i) and angular error (δ_ψ^i, δ_φ^i, δ_θ^i) in the i-th fraction (i = 2, 3, 4, …) were calculated as

$$\delta_q^i = v_q^i - v_q^1, \quad (2)$$

where q is each component of translation (x, y, z) or rotation (ψ, ϕ, θ) and v^1 is relative couch position or angular difference in the first fraction after acquisition of the planning CT. Since virtual couch position is usually based on the planning CT, we should have compared positional information in each fraction with that at planning. However, because of the lack of alignment logfiles at planning CT acquisition, we instead used relative couch position and angular difference in the first fraction after acquisition of planning CT. L2 norm of translational error and angular error was also calculated. The L2 norm of a vector (x_1, x_2, x_3) can be calculated as $(x_1^2 + x_2^2 + x_3^2)^{1/2}$. Positional errors were compared using the Wilcoxon signed-rank test, all p values were two-side and those < 0.01 were regarded at statistically significant. All evaluations were performed using commercial software (MATLAB R2017a®, MathWorks, Natick, MA, USA).

2.3. Dose assessment

To estimate the dosimetric impact of the patient positional variation on the treatment couch, we compared plans according to 4 scenarios, namely no translational error, average translational error, 95th percentile translational error, and maximum translational error scenarios. Twenty-eight patients were randomly chosen from those receiving prostate, bone and soft tissue sarcoma, head and neck, rectum, liver, lung, and pancreas treatment (4 patients × 7 treatment sites). First, we performed treatment plans in the no translational error scenario. All clinical target volumes (CTVs) were delineated by experienced radiation oncologists. For prostate treatment, planning target volumes (PTVs) were created by adding a 10-mm margin in the patient's right, left, and anterior directions and a 5-mm margin to the CTVs [14]. For treatment sites with respiratory motion (liver, lung, and pancreas), CTVs were delineated on peak exhale phase CT image in four-dimensional computed tomography (4DCT) images. As for our clinical protocols, scanned carbon-ion beam is irradiated with respiratory gating. Treatment beam is turned on when a respiratory signal is lower than the gating threshold. This threshold is determined so that the respiratory-induced tumor motion is smaller than 2 mm while the beam is on. Because tumor moves mainly along superior-inferior direction, we added a 2-mm margin in the patient's inferior direction to compensate respiratory motion. We added additional 1-mm margin in all directions for compensating inter-fractional organ variations and created an internal target volume (ITV). PTVs were created from the ITVs by adding

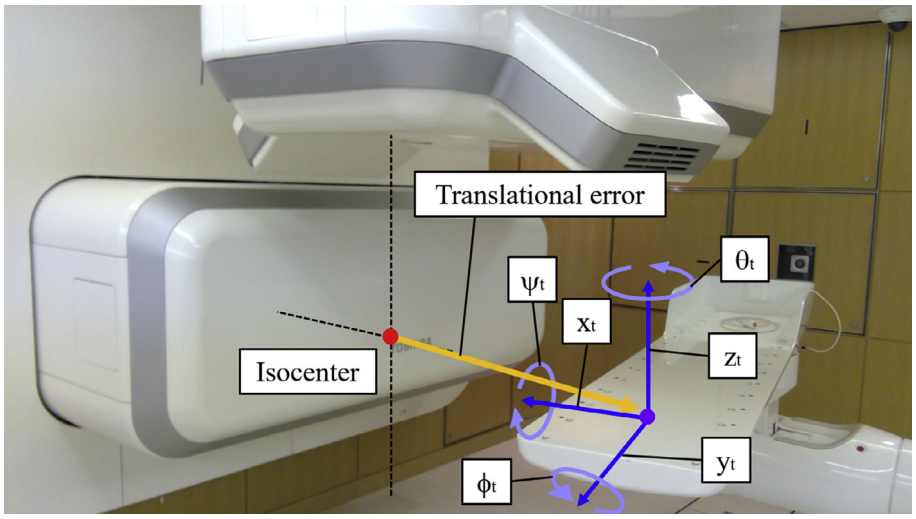

Fig. 1. Blue and pale blue arrows represent each axis of table top coordinate system (x_t, y_t, z_t, ψ_t, φ_t, and θ_t) defined by the IEC [13]. Red and purple dots show isocenter and the origin of the table top coordinate system, respectively. Translational error was defined as a vector from isocenter to the origin of the table top coordinate system (orange arrow). (For interpretation of the references to colour in this figure legend, the reader is referred to the web version of this article.)

a 2-mm margin to account for setup error. For the other treatment sites (bone and soft tissue sarcoma, head and neck, rectum), a 2-mm setup margin was added to the CTVs to create PTVs.

Gantry angles were determined to avoid having the treatment beam pass through a supporting bar. Since two supporting bars (Fig. 2) had the highest relative stopping power among all structures in the treatment couch, these bars can cause significant dosimetric changes. The bars were therefore contoured and their relative stopping power was replaced with 1.15 au. The distance between the couch bar and the outer edge of the treatment beam passing through the PTV was 10 mm on the isocenter plane (Fig. 2). In other words, the margin of the PTV and the bar observed in a beam's eye view was 10 mm. We used single-field optimization [15] to create a uniform dose distribution in the PTV. Spot spacing was 2 mm. The lateral margin was 2 mm to compensate for the lateral beam penumbra. Energy layer spacing was 0.2 g/cm^2. The proximal margin and distal margin were both 0.2 g/cm^2.

Second, the other scenarios were simulated by shifting the treatment couch along the patient's left or right side so that the supporting bar approached the treatment beam axis. The left-right direction was the worst direction in terms of the interference between the bar and the treatment beam. Mean value, 95th percentile value, and maximum value of the translational errors in the x_t-direction (patient's left-right direction) were calculated for each treatment site. The treatment couch was shifted by above scenarios. Each dose distribution was then recalculated without any change in the plan parameters. A total of 112 dose distributions (=7 treatment sites × 4 patients × 4 scenarios) were calculated. Dose volume parameters for PTV, CTV, and organs at risk were calculated with each couch shift. All simulations were performed using RayStation 7 (RaySearch Laboratories AB, Stockholm, Sweden).

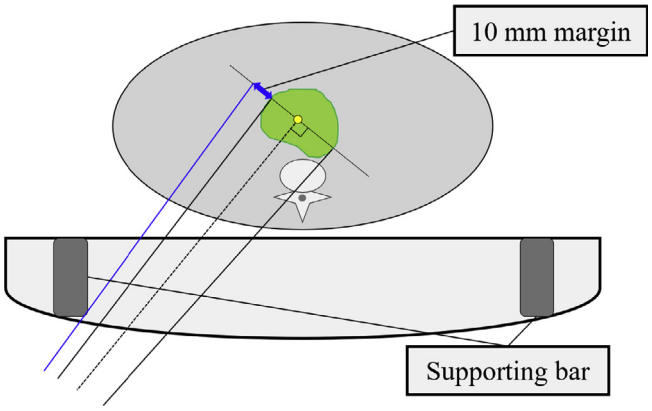

Fig. 2. A schematic drawing of the treatment couch, patient and treatment beam configurations. Black dotted line is the central beam axis to the target isocenter (yellow dot). Black solid lines show the beam edge. The gap between outer beam edge and a couch supporting bar was 10 mm on isocenter plane. (For interpretation of the references to colour in this figure legend, the reader is referred to the web version of this article.)

3. Results

3.1. Patient positional reproducibility

Fig. 3 shows the histograms for translational error and angular error. The histograms were all symmetrical and mean values were close to zero. Table 2 shows a summary of the absolute values of translational error and angular error. In all treatment sites, translational error was smaller in the z_t-direction than in the other directions. We found large translational errors in prostate, liver, and pancreas treatment (mean values were 8.0 mm, 7.4 mm, and 6.5 mm in L2 norm), as well as small translational errors in head and neck treatment, lung treatment over 4 fractions, and lung treatment over 12 fractions (mean values were 3.2 mm, 4.1 mm, and 4.2 mm, respectively). Bone and soft tissue and rectum patients showed intermediate translational errors (SD values were 5.6 mm and 4.8 mm, respectively).

To clarify the inter-fractional changes in translational error, we calculated the variation of L2 norm of translational error during treatment courses (Fig. 4). Data for representative treatment sites, such as prostate, head and neck, and bone and soft tissue, are shown in this figure. There were no statistically significant differences between the first fraction and the last fraction in prostate (p = 0.302), head and neck (p = 0.181), and bone and soft tissue (p = 0.882) using the Wilcoxon rank sum test. In prostate and head and neck treatment, the translational errors in even fractions were slightly larger than those in odd fractions. The tendency was not found in bone and soft tissue treatment.

Fig. 5 shows translational and angular errors for a prostate case. This case showed the largest standard deviation in translational error (10.5 mm, 4.6 mm, and 2.9 mm in x_t, y_t, and z_t-directions, respectively). The maximum value of translational error was 28.2 mm in the x_t-direction. The mean translational error in the x_t-direction in odd fractions (= −23.0 mm) was larger than that in the even fractions (=4.3 mm) in this case (p < 0.01).

3.2. Dose assessment

Example dose distributions of pancreatic treatment in the no translational error scenario, average translational error scenario, 95th

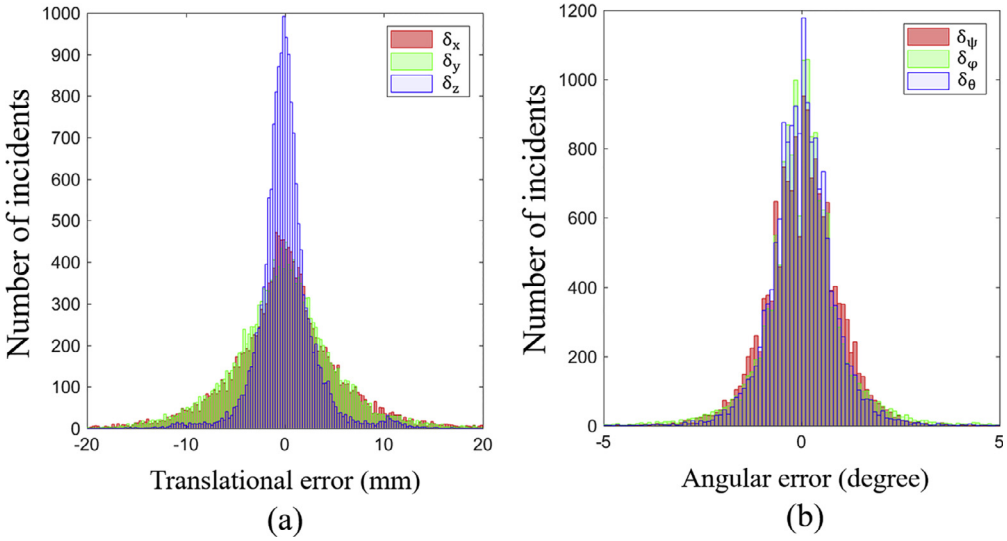

Fig. 3. Patient positional error for all patients in (a) translation and (b) rotation.

percentile translational error scenario, and maximum translational error scenario are depicted in Fig. 6a–d, respectively. A significant change in the dose-volume histogram curve for the first to second portion of the duodenum (D1-2) was found in this patient (Fig. 7). Minimum dose in the most exposed 2 cc volume (D2cc) for D1-2 was 55.2%, 55.2%, 55.2%, 83.0% in the no, average, 95th percentile, and maximum translational error scenarios, respectively. The shortened beam range resulted from interference between the bar and the couch. As a result, under-dosage distal to the PTV and over-dosage proximal to the PTV were observed (Fig. 6e–g). While there were no significant dosimetric changes in the average translational error scenario (Fig. 6e), significant changes were found in the 95th percentile translational error (Fig. 6f) and maximum translational error scenarios (Fig. 6g).

Table 3 summarizes the changes in dose-volume metrics due to the couch shift in each scenario. Although in this study we also calculated D2cc in the rectum in prostate treatment and ipsilateral eye/optic nerve in head and neck treatment; Dmax in the spinal cord in pancreas treatment; and the minimum dose covering 95% of the volume (D95) in CTV in all treatment sites, these values are omitted from this table because the difference was quite small ($< 0.5\%$) in all patients. In the average translational error scenario, no or only small changes were seen in dose-volume metrics. In the 95th percentile translational error scenario, maximum dose (Dmax) in the chiasma and D2cc in D1-2 were slightly changed due to the couch shift on average, the maximum difference values were significant. In the maximum translational error scenario, significant changes were observed in PTV-D95 (prostate treatment), D1-2-D2cc, and intestine-D2cc (pancreas treatment). It should be noted that since a huge number of patients with prostate cancer were included, their maximum translational error was large ($= 32.0$ mm in x_t-direction) compared to those at the other treatment sites. This large translational error was applied in this scenario, albeit that it is considered to be extremely rare.

4. Discussion

We evaluated the translational error and angular error from the treatment couch positions in 7 treatment sites with 1023 patients. We also estimated its effect on dose distribution in 28 patients of 7 treatment sites. The L2 norm of translational error was > 15 mm in 5% of treatment fractions and maximized at 30 mm, which can cause a significant change in dose distribution and dose-volume parameters to OARs. The translational error showed an obvious dependency on treatment sites. The dependency would be mainly caused by different immobilization devices. For example, we had used thermoplastic shells to tightly fix head, neck, and shoulders in head and neck treatments. Shoulders and arms of lung cancer patients were also fixed by a

Table 2
Summary of absolute translational error and absolute angular error. Data are expressed as mean ± standard deviation (95th percentile, maximum).

Treatment site	Prostate	B&S	H&N	Rectum	Liver	Lung (4 Fr)	Lung (12 Fr)	Pancreas	Combined
|δx| (mm)	4.9 ± 4.2 (12.9, 32.0)	2.7 ± 3.0 (8.4, 23.0)	1.7 ± 1.6 (5.2, 10.1)	1.9 ± 2.5 (5.2, 21.0)	4.1 ± 3.3 (10.2, 14.9)	2.4 ± 2.5 (8.0, 8.3)	2.3 ± 1.9 (6.5, 8.1)	3.4 ± 3.5 (9.9, 20.8)	4.0 ± 3.9 (11.7, 32.0)
|δy| (mm)	4.5 ± 3.9 (12.1, 46.2)	3.5 ± 3.3 (10.2, 23.0)	1.8 ± 1.6 (5.0, 8.3)	3.4 ± 2.8 (8.5, 17.3)	5.2 ± 3.4 (11.4, 12.4)	2.5 ± 2.3 (7.7, 7.9)	2.2 ± 1.8 (6.1, 9.7)	4.0 ± 4.5 (14.0, 25.7)	3.9 ± 3.7 (11.2, 46.2)
|δz| (mm)	2.1 ± 2.3 (6.8, 17.4)	1.9 ± 1.7 (4.8, 13.4)	1.1 ± 1.0 (3.2, 7.7)	1.5 ± 2.3 (3.4, 18.6)	1.5 ± 1.4 (4.5, 4.8)	1.0 ± 0.9 (3.4, 3.6)	1.8 ± 1.6 (5.3, 8.4)	1.6 ± 1.4 (4.4, 7.1)	1.9 ± 2.1 (5.8, 18.6)
L2 norm (mm)	8.0 ± 4.6 (16.4, 46.3)	5.6 ± 3.8 (12.7, 24.9)	3.2 ± 1.8 (6.8, 11.2)	4.8 ± 3.7 (10.7, 25.8)	7.4 ± 3.8 (14.2, 16.6)	4.1 ± 2.9 (9.3, 9.3)	4.2 ± 2.3 (8.5, 11.2)	6.5 ± 4.7 (17.5, 27.1)	6.9 ± 4.6 (15.6, 46.3)
|δψ| (degree)	0.6 ± 0.5 (1.7, 4.1)	0.8 ± 0.8 (2.4, 5.0)	0.8 ± 0.7 (2.2, 4.1)	0.7 ± 0.6 (1.9, 4.5)	0.5 ± 0.4 (1.3, 1.5)	0.9 ± 0.7 (2.1, 2.2)	0.5 ± 0.5 (1.4, 2.0)	0.6 ± 0.5 (1.6, 3.9)	0.7 ± 0.6 (1.8, 5.0)
|δφ| (degree)	0.5 ± 0.4 (1.2, 3.3)	1.1 ± 1.1 (3.1, 8.2)	1.2 ± 1.0 (3.1, 7.3)	1.0 ± 1.0 (3.1, 6.0)	0.7 ± 0.5 (1.6, 1.8)	0.9 ± 0.7 (2.1, 2.1)	1.0 ± 0.9 (2.9, 3.6)	0.7 ± 0.7 (2.0, 4.7)	0.7 ± 0.7 (2.0, 8.2)
|δθ| (degree)	0.5 ± 0.4 (1.3, 2.9)	0.5 ± 0.5 (1.5, 2.9)	1.0 ± 0.9 (2.7, 6.5)	0.6 ± 0.5 (1.6, 2.8)	0.4 ± 0.3 (1.1, 1.2)	0.6 ± 0.4 (1.5, 1.6)	0.6 ± 0.5 (1.5, 2.0)	0.7 ± 0.6 (1.9, 2.9)	0.6 ± 0.6 (1.6, 6.5)
L2 norm (degree)	1.1 ± 0.6 (2.1, 5.1)	1.7 ± 1.1 (4.1, 8.4)	2.0 ± 1.1 (4.3, 9.0)	1.6 ± 0.9 (3.5, 6.0)	1.1 ± 0.5 (2.1, 2.6)	1.6 ± 0.8 (2.7, 2.7)	1.4 ± 0.9 (3.2, 3.9)	1.4 ± 0.8 (2.7, 5.0)	1.3 ± 0.8 (2.8, 9.0)

Abbreviation = B&S: bone and soft tissue sarcoma, H&N: head and neck, L2 norm of a vector (x_1, x_2, x_3): $(x_1^2 + x_2^2 + x_3^2)^{1/2}$.

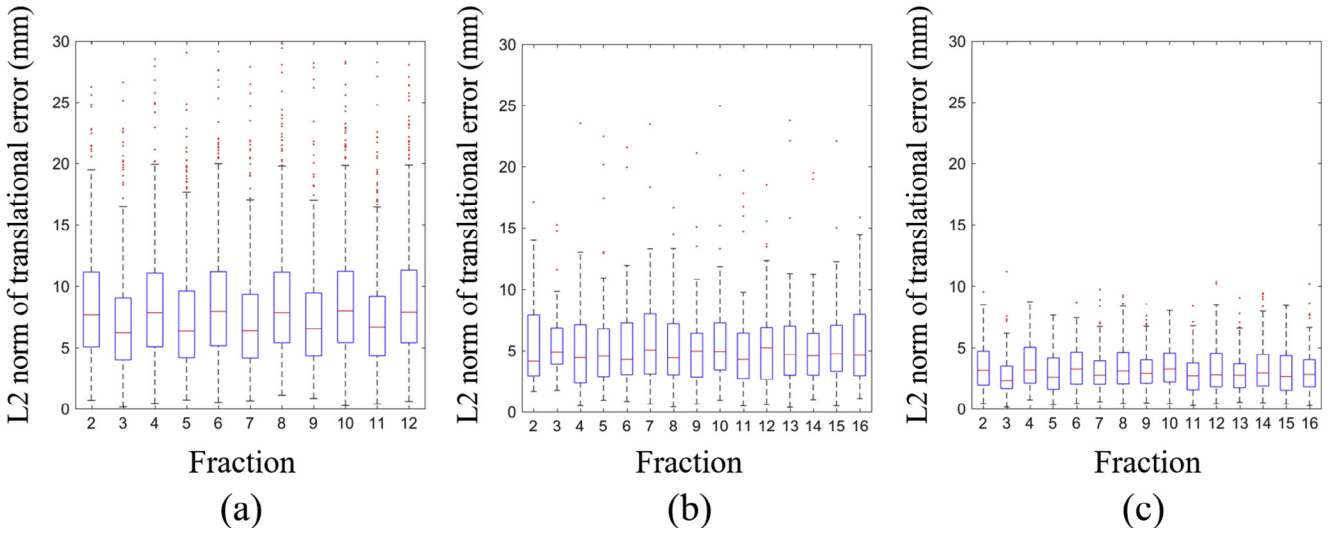

Fig. 4. L2 norm of translational error in respective treatment fractions for (a) prostate, (b) bone and soft tissue sarcomas, and (c) head and neck treatment. The L2 norm of a vector (x_1, x_2, x_3) was calculated as $(x_1^2 + x_2^2 + x_3^2)^{1/2}$. The central red mark indicates the median, and the bottom and top edges of the box indicate the 25th percentiles (q_1) and 75th percentiles (q_3), respectively. The whiskers extend to the most extreme data points not considered outliers. Outliers (red dots) were identified if they were $> q_3 + (q_3 - q_1) \times 1.5$ or less than $q_1 - (q_3 - q_1) \times 1.5$.

hydraulic urethane resin cushion. These immobilization devices were assumed to result in the small translational error in head and neck and lung treatment.

The influence on dose distributions from angular error is a little complicated. When the treatment couch is rotated, the movement of couch bars gets larger as it goes away from the center of rotation (the origin of the table top coordinate system). The distance between the center of rotation and the farthest point in the bars was 20 cm. Couch rotation of 0.7 degrees (mean value of $|\delta_\varphi|$ in Table 2) correspond to a shift of 2.4 mm at 20 cm away from the rotation center. Because this was smaller than the mean value of $|\delta_x|$, translational error along x_t-direction will have more significant influence than the angular error.

We found that the translational errors were slightly larger in even fractions than odd fractions in prostate and head and neck treatment. In prostate treatment, patients were alternately irradiated from the right and left sides. Because we used a fixed beam port, the treatment couch was alternately set as $\theta_t = 0$ degrees and 180 degrees. If $\theta_t = 0$ degrees, patients have to board the treatment couch from its left side (negative direction on the x_t-axis), but from its right side (positive direction on the x_t-axis) when $\theta_t = 180$ degrees. The difference in how the patients boarded the treatment couch may have produced large variations in patient setup. In head and neck treatment, patients were alternately rotated in the ϕ_t-direction. Gravity may have affected the relative position between the couch and the patient in even fractions. However, the effect from the other factors, such as patient's performance status, age, obesity, proficiency of technicians, is still unclear.

There are many studies of set-up uncertainty with several immobilization and positioning methods. Baumert et al. and Russo et al. [16,17] reported the improvement of set-up accuracy by a maxillary fixation device or a bite-block. White et al. [18] also reported the high reproducibility of the whole-body immobilization system compared to immobilization of the hips and legs. Because we did not use a maxillary fixation device or a bite-block or a whole-body immobilization device, further reduction of positioning uncertainty might be possible using these immobilization devices. The matching method [19], patient positioning [20], and image artifacts from metal structures [21] could also

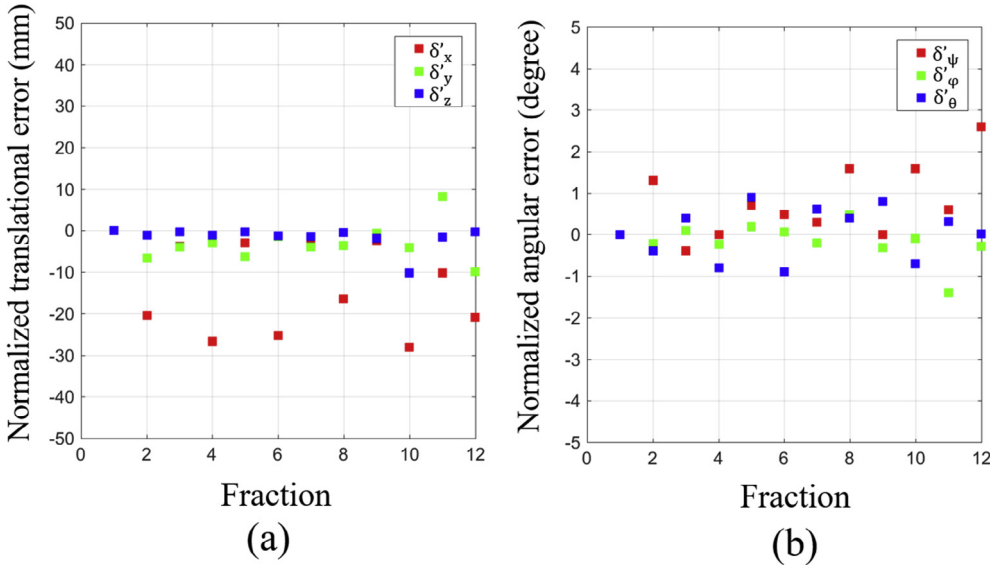

Fig. 5. Translational error for each fraction (a) and angular error for each fraction (b) for the prostate treatment (patient no. 54).

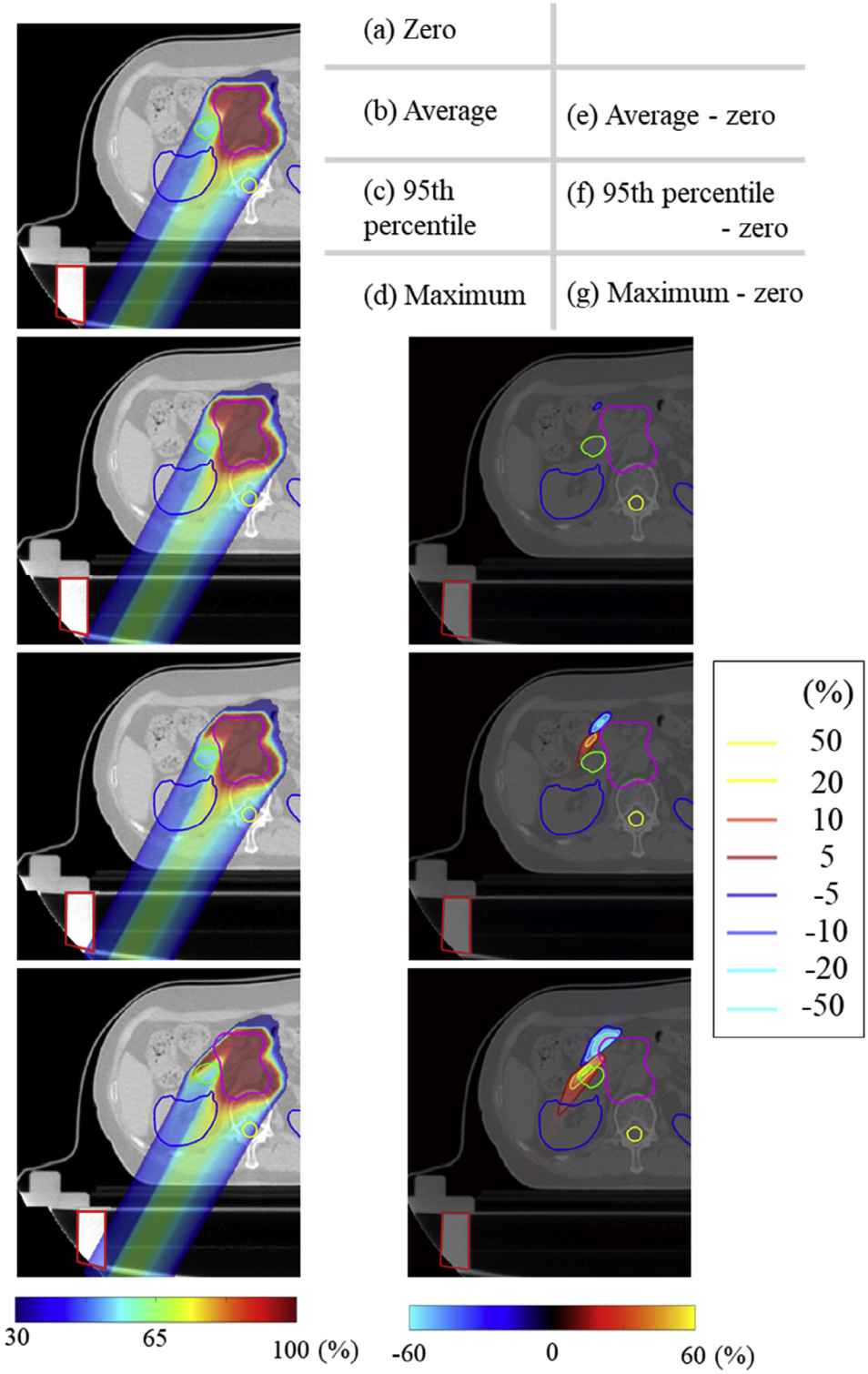

Fig. 6. Dose distributions in the no translational error scenario (a), average translational error scenario (b), 95th percentile translational error scenario (c), and maximum translational error scenario (d). Dose difference maps were calculated by subtracting the dose in the no translational error scenario from the dose in the average (e), 95th percentile (f), and maximum (g) translational error scenarios. Magenta, green, blue, yellow, and red contours represent PTV, D1-2, kidneys, spinal cord, and supporting bars, respectively.

affect the uncertainty of the relative position between the patient and the treatment couch.

Since the translational error or angular error value in the first fraction was used for normalization, the difference of these errors between acquisition of the planning CT and the first fraction was ignored. Because even trivial things, such as how the patient boarded the treatment couch, influenced these errors, the results might be changed if positional information at acquisition of the planning CT was used for normalization.

According to our simulation with three different couch shifts, a centimeter margin between a couch supporting bar and PTV could avoid significant underdosage to the PTV in most scenarios and

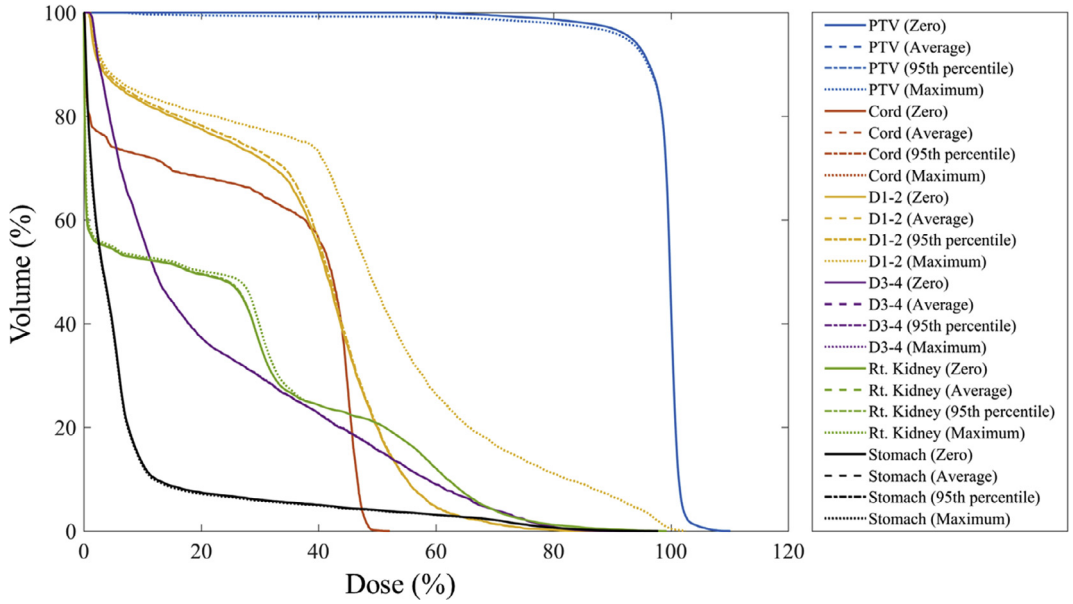

Fig. 7. Dose-volume histograms for respective targets and organs at risk. Histograms in the no, average, 95th percentile, and maximum translational error scenarios are depicted as solid, dashed, dash-dot, and dotted lines, respectively.

treatment sites, while an extremely large translational error might degrade the PTV dose coverage. D95 values in the CTV were maintained in all patients and scenarios. A centimeter is a reasonable value because it is comparable to usual internal and set-up margin [22–25]. However, a centimeter margin was not enough to avoid the significant overdosage to some organs at risk, such as the chiasma and D1-2 in 95th percentile translational error scenario and many organs at risk in the maximum translational error scenario.

The dosimetric effect from the high stopping power materials in the treatment couch differed significantly, depending on patients. For example, in rectum treatment, D2cc value in the intestine was increased by 21.7% for one patient, but decreased by 4.7% for another. The positions of the OARs and PTV can explain the differences. High stopping power materials act as a range shifter, as they interfere with the treatment beam and shorten the beam range. Therefore, unexpected over-dosage appears in the region proximal to the PTV. If OARs are present in that region, the effect of the high stopping power materials should be carefully controlled. An additional margin in the beam's eye view or appropriate selection of gantry angles can reduce this potential risk. There are some limitations in this study due to a simplified

Table 3
Summary of dose-volume parameter changes with each couch shift. Dose-volume parameters with each couch shift (average, 95th percentile, and maximum couch shift) were subtracted from those without couch shift. Data are expressed as mean difference (minimum difference, maximum difference). All data is given in units of %.

Treatment site	Volume	Metric	Couch shift		
			average	95th percentile	maximum
Prostate	PTV	D95	0.0 (0.0, 0.0)	0.0 (0.0, 0.0)	−37.6 (−78.7, −2.9)
B&S	PTV	D95	0.0 (0.0, 0.0)	0.0 (0.0, 0.0)	0.0 (0.0, 0.0)
	Rectum	D2cc	0.0 (0.0, 0.0)	0.0 (0.0, 0.0)	4.7 (0.0, 13.7)
H&N	PTV	D95	0.0 (0.0, 0.2)	0.0 (0.0, 0.2)	0.0 (0.0, 0.2)
	Chiasma	Dmax	0.0 (0.0, 0.0)	1.0 (0.0, 4.1)	2.7 (0.0, 10.9)
	Brainstem	D2cc	0.0 (0.0, 0.1)	0.4 (0.0, 0.7)	1.8 (0.0, 4.3)
	Contralateral eye	Dmax	0.0 (0.0, 0.0)	0.0 (-0.1, 0.0)	−0.1 (-0.2, 0.0)
	Contralateral optic nerve	Dmax	0.0 (0.0, 0.0)	−0.1 (-0.2, 0.0)	−0.2 (-0.6, 0.0)
Rectum	PTV	D95	0.0 (0.0, 0.0)	0.0 (0.0, 0.0)	−0.2 (-0.6, 0.0)
	Intestine	D2cc	0.0 (0.0, 0.0)	0.0 (-0.1, 0.1)	4.5 (-4.7, 21.7)
Liver	PTV	D95	0.0 (0.0, 0.0)	0.0 (0.0, 0.0)	0.0 (0.0, 0.0)
	Liver	V20	0.0 (0.0, 0.0)	0.0 (-0.1, 0.0)	0.0 (-0.2, 0.1)
Lung	PTV	D95	0.0 (0.0, 0.0)	0.0 (0.0, 0.0)	0.0 (0.0, 0.0)
	Ipsilateral lung	V20	0.0 (0.0, 0.0)	0.0 (0.0, 0.0)	0.0 (0.0, 0.1)
Pancreas	PTV	D95	0.0 (0.0, 0.0)	0.0 (0.0, 0.0)	−0.4 (-0.9, −0.1)
	D1-2	D2cc	0.0 (0.0, 0.1)	1.8 (0.0, 6.5)	21.7 (10.0, 27.9)
	D3-4	D2cc	0.0 (0.0, 0.0)	0.0 (0.0, 0.0)	0.7 (0.0, 2.8)
	Right kidney	V20	0.6 (0.0, 1.7)	1.2 (0.3, 2.3)	4.1 (1.5, 8.1)
	Stomach	D2cc	0.0 (0.0, 0.0)	0.0 (0.0, 0.0)	−1.5 (0.0, 0.0)
	Intestine	D2cc	0.4 (0.0, 1.3)	1.0 (0.0, 1.8)	−9.8 (-18.2, 0.0)

Abbreviation = B&S: bone and soft tissue sarcoma, H&N: head and neck, D1-2: First and second portion of the duodenum, D3-4: Third and fourth portion of the duodenum.

simulation: a shift only along the x-direction and irradiation with one port. It is necessary to consider these factors for more accurate estimation of the influence of setup variations.

5. Conclusion

We presented an evaluation study of the positional reproducibility in patient setup and its impact on dose distribution. The 95th percentile value of the setup variation was 15 mm. We have to take it into account in treatment planning process. The translational error depended on treatment site, probably because of the different immobilization devices for each treatment site. Although a 1 cm margin in the beam's eye view could avoid significant underdosage to the PTV for a pancreatic patient, the dose to OARs might increase. Further improvement in immobilization technique would reduce the setup variation.

Acknowledgments

We thank Libby Cone, MD, MA, from DMC Corp. (www.dmed.co.jp) for editing drafts of this manuscript. We also thank RaySearch Laboratories AB for providing RayStation used for treatment planning in this study.

Funding: This research received no specific grant from any funding agency in the public, commercial, or not-for-profit sectors.

Appendix

Consider a table top coordinate system having three orthogonal axes (x_t, y_t, and z_t). The direction of these axes are defined by IEC 61217 [13]. Here we describe the extent of couch translation along the x_t, y_t, and z_t-axes as x, y, and z, respectively; and couch rotation about the x_t, y_t, and z_t-axes as ψ, ϕ, and θ, respectively (Fig. 1). These quantities were recorded in logfiles of the patient alignment system. If all these values were zero ($x = y = z = \psi = \phi = \theta = 0$), the origin of a table top coordinate system corresponds to isocenter. When any of these values are not zero, a table top coordinate system is transformed in the following order:

First, rotation about the z_t axis by an angle θ is applied. The table top coordinate system after the rotation (x_t', y_t', z_t') can be calculated from the coordinate system before the rotation (x_t, y_t, z_t) as

$$\begin{pmatrix} x_t' \\ y_t' \\ z_t' \\ 1 \end{pmatrix} = A_\theta \begin{pmatrix} x_t \\ y_t \\ z_t \\ 1 \end{pmatrix}, \tag{3}$$

where three-dimensional rotation matrix A_θ, which represents a rotation about z_t-axis, is given by

$$A_\theta = \begin{pmatrix} \cos\theta & \sin\theta & 0 & 0 \\ -\sin\theta & \cos\theta & 0 & 0 \\ 0 & 0 & 1 & 0 \\ 0 & 0 & 0 & 1 \end{pmatrix}. \tag{4}$$

Second, translation along the x_t', y_t', and z_t' axes by amounts x, y, and z is applied, respectively. The relationship between table top coordinate system before the translation (x_t', y_t', z_t') and after the translation (x_t'', y_t'', z_t'') can be expressed as

$$\begin{pmatrix} x''_t \\ y''_t \\ z''_t \\ 1 \end{pmatrix} = A_T \begin{pmatrix} x'_t \\ y'_t \\ z'_t \\ 1 \end{pmatrix}, \tag{5}$$

where translation matrix A_T is given by

$$A_T = \begin{pmatrix} 1 & 0 & 0 & -x \\ 0 & 1 & 0 & -y \\ 0 & 0 & 1 & -z \\ 0 & 0 & 0 & 1 \end{pmatrix}. \tag{6}$$

Third, rotation about the x_t"-axis by an angle ψ is applied. The couch top coordinate system after the rotation (x_t''', y_t''', z_t''') is calculated as

$$\begin{pmatrix} x_t''' \\ y_t''' \\ z_t''' \\ 1 \end{pmatrix} = A_\psi \begin{pmatrix} x_t'' \\ y_t'' \\ z_t'' \\ 1 \end{pmatrix}, \tag{7}$$

where rotation matrix A_ψ is

$$A_\psi = \begin{pmatrix} 1 & 0 & 0 & 0 \\ 0 & \cos\phi & \sin\phi & 0 \\ 0 & -\sin\phi & \cos\phi & 0 \\ 0 & 0 & 0 & 1 \end{pmatrix}. \tag{8}$$

Finally, rotation about the y_t'''-axis by an angle ϕ is applied. The table top coordinate system after the rotation (x_t'''', y_t'''', z_t'''') is expressed as

$$\begin{pmatrix} x_t'''' \\ y_t'''' \\ z_t'''' \\ 1 \end{pmatrix} = A_\phi \begin{pmatrix} x_t''' \\ y_t''' \\ z_t''' \\ 1 \end{pmatrix}, \tag{9}$$

where rotation matrix A_ϕ is

$$A_\varphi = \begin{pmatrix} \cos\phi & 0 & -\sin\phi & 0 \\ 0 & 1 & 0 & 0 \\ \sin\phi & 0 & \cos\phi & 0 \\ 0 & 0 & 0 & 1 \end{pmatrix}. \quad (10)$$

We can obtain the isocenter position in the transformed table top coordinate system (x_t'''', y_t'''', z_t'''') by substituting (x_t, y_t, z_t) = (0,0,0) and summarizing Eqs. (3)–(10). Eq. (1) can be then derived by multiplying by -1 because translational error is defined by a vector from the isocenter to the origin of the transformed table top coordinate system.

References

[1] Giap H, Giap B. Historical perspective and evolution of charged particle beam therapy. Trans. Cancer Res. 2012;1:127–36.
[2] Barendsen GW. Differences between biological effects of high LET and low LET radiations in relation to their application in radiotherapy. Radiol. Clin. (Basel) 1977;46:380–9.
[3] Bragg WH, Kleeman RLXXIV. On the ionization curves of radium. Lond. Edinb. Dubl. Phil. Mag. 1904;8:726–38.
[4] Smith A, Gillin M, Bues M, Zhu XR, Suzuki K, Mohan R, et al. Anderson proton therapy system. Med. Phys. 2009;36:4068–83.
[5] Haberer T, Debus J, Eickhoff H, Jakel O, Schulz-Ertner D, Weber U. The Heidelberg ion therapy center. Radiother. Oncol. 2004;73(Suppl 2):S186–90.
[6] Iwata Y, Fujimoto T, Matsuba S, Fujita T, Sato S, Furukawa T, et al. Beam commissioning of a superconducting rotating-gantry for carbon-ion radiotherapy. Nucl. Instrum. Meth. Phys. Res A 2016;834:71–80.
[7] Zhao T, Sun B, Grantham K, Rankine L, Cai B, Goddu SM, et al. Commissioning and initial experience with the first clinical gantry-mounted proton therapy system. J. Appl. Clin. Med. Phys. 2016;17:24–40.
[8] Iwata Y, Noda K, Murakami T, Shirai T, Furukawa T, Fujita T, et al. Development of a superconducting rotating-gantry for heavy-ion therapy. Nucl. Instrum. Meth. Phys. Res. B 2013;317:793–7.
[9] Yoon M, Kim J, Ahn S, Cheong M, Lim Y, Kim D, et al. SU-FF-T-477: study on the modeling of digital couch for proton treatment planning system. Med. Phys. 2009;36:2632–3.
[10] Yu Z, Bluett J, Zhang Y, Zhu X, Lii M, Mohan R, et al. SU-FF-T-470: impact of daily patient setup variation on proton beams passing through the couch edge. Med. Phys. 2010;37:3294-.
[11] Mori S, Shirai T, Takei Y, Furukawa T, Inaniwa T, Matsuzaki Y, et al. Patient handling system for carbon ion beam scanning therapy. J. Appl. Clin. Med. Phys. 2012;13:3926.
[12] Mori S, Kumagai M, Miki K, Fukuhara R, Haneishi H. Development of fast patient position verification software using 2D–3D image registration and its clinical experience. J. Radiat. Res. 2015;56:818–29.
[13] IEC: International Electrotechnical Commission. Radiotherapy equipment: coordinates, movements and scales. IEC 61217, 2008.
[14] Michalski JM, Yan Y, Watkins-Bruner D, Bosch WR, Winter K, Galvin JM, et al. Preliminary toxicity analysis of 3-dimensional conformal radiation therapy versus intensity modulated radiation therapy on the high-dose arm of the Radiation Therapy Oncology Group 0126 prostate cancer trial. Int. J. Radiat. Oncol. Biol. Phys. 2013;87:932–8.
[15] Lomax A. Intensity modulation methods for proton radiotherapy. Phys. Med. Biol. 1999;44:185–205.
[16] Baumert BG, Egli P, Studer S, Dehing C, Davis JB. Repositioning accuracy of fractionated stereotactic irradiation: assessment of isocentre alignment for different dental fixations by using sequential CT scanning. Radiother. Oncol. 2005;74:61–6.
[17] Russo M, Owen R, Bernard A, Moutrie V, Foote M. Evaluation of accuracy and reproducibility of a relocatable maxillary fixation system for fractionated intracranial stereotactic radiation therapy. J. Med. Radiat. Sci. 2016;63:41–7.
[18] White P, Yee CK, Shan LC, Chung LW, Man NH, Cheung YS. A comparison of two systems of patient immobilization for prostate radiotherapy. Radiat. Oncol. 2014;9:29.
[19] Abe S, Kubota Y, Shibuya K, Koyama Y, Abe T, Ohno T, et al. Fiducial marker matching versus vertebral body matching: dosimetric impact of patient positioning in carbon ion radiotherapy for primary hepatic cancer. Phys. Med. 2017;33:114–20.
[20] Miki K, Fukahori M, Kumagai M, Yamada S, Mori S. Effect of patient positioning on carbon-ion therapy planned dose distribution to pancreatic tumors and organs at risk. Phys. Med. 2016.
[21] Mastella E, Molinelli S, Magro G, Mirandola A, Russo S, Vai A, et al. Dosimetric characterization of carbon fiber stabilization devices for post-operative particle therapy. Phys. Med. 2017;44:18–25.
[22] Meijer GJ, de Klerk J, Bzdusek K, van den Berg HA, Janssen R, Kaus MR, et al. What CTV-to-PTV margins should be applied for prostate irradiation? Four-dimensional quantitative assessment using model-based deformable image registration techniques. Int. J. Radiat. Oncol. Biol. Phys. 2008;72:1416–25.
[23] Riou O, Serrano B, Azria D, Paulmier B, Villeneuve R, Fenoglietto P, et al. Integrating respiratory-gated PET-based target volume delineation in liver SBRT planning, a pilot study. Radiat. Oncol. 2014;9:127.
[24] Liang J, Li M, Zhang T, Han W, Chen D, Hui Z, et al. The effect of image-guided radiation therapy on the margin between the clinical target volume and planning target volume in lung cancer. J. Med. Radiat. Sci. 2014;61:30–7.
[25] Gadia R, Leite ET, Gabrielli FG, Marta GN, Arruda FF, Abreu CV, et al. Outcomes of high-dose intensity-modulated radiotherapy alone with 1 cm planning target volume posterior margin for localized prostate cancer. Radiat. Oncol. 2013;8:285.